Use of Moringa Oleifera Seeds as a Biosorbent and Antimicrobial Agent in Acidic Mineral Effluents

Pauline Ncube (ppncube01@gmail.com)
University of Johannesburg - Doornfontein Campus https://orcid.org/0000-0002-5468-5450
Freeman Ntuli
University of Johannesburg - Doornfontein Campus
Thabo Falayi
Malawi University of Science and Technology

Research Article

Keywords: environmental pollution, water treatment, Moringa oleifera, Acid Mine Drainage, biosorbent, antimicrobial agent

Posted Date: August 13th, 2021

DOI: https://doi.org/10.21203/rs.3.rs-794787/v1

Abstract

Moringa Oleifera (MO) seed extract was used as an antimicrobial agent and a biosorbent to remove heavy metals from acidic mineral effluents. Biosorption experiments were conducted in a thermostatic shaker using synthetic acidic mineral effluent(SAME) of composition, 20 ppm, 20 ppm, 100 ppm, and 500 ppm for Ni, Cu, Mn, and Fe, respectively. The Quanti-tray and SimPlate standard procedures were used for the antimicrobial tests. The aqueous seed extract achieved microbial reductions of 100% total coliform and 90.5% Heterotrophic Plate Count (HPC). Ni and Cu were the most removed metals and optimum sorption conditions achieved were pH = 3, Temperature = 308 K, solid loading = 10% m/v, and residence time = 90 minutes. The biosorption process was endothermic for all the metals but only feasible and spontaneous for Cu and Ni. The Langmuir model and second-order kinetics best fit the adsorption process for Ni, Cu, and Fe, while ion-exchange/ chemisorption was the possible mechanism of adsorption. Overall, MO seed extract was an effective antimicrobial agent and bio-sorbent for Ni, Cu, and Fe removal in acidic mineral effluent. The use of MO in acidic medium is a novel technique.

1 Introduction

Water is an essential basic commodity for life. Lack of safe drinking water is mainly due to water contamination in rivers and dams caused by continued growth in industrial and urban centers. Heavy metal pollution from mining, milling, electroplating, and surface finishing industries often results in acidic mineral effluents such as acid mine drainage (AMD), which discharges a range of toxic metals, including Fe, Cu, Ni, Mn, Pb, and Co into the environment. Thus, AMD-contaminated water poses a considerable threat to the environment. The water could channel its way into the ecosystem, causing pollution in surface water and subsequently groundwater close to the mining areas, whether active or abandoned. Heavy metals, unlike organic pollutants, are non-biodegradable and can accumulate in living tissue resulting in adverse health problems (Zhang, 2011).

Consequently, heavy metal removal from acidic mineral effluents such as AMD has been one of the major global concerns for years. In South Africa, the Gauteng region has been classified as a top priority area requiring immediate action due to the vast environmental impact of AMD and lack of adequate measures to address it (Inter-Ministerial Report, 2010). Traditionally, the treatment of AMD involves neutralization with limestone ($CaCO_3$) or slaked lime ($Ca(OH)_2$), giving rise to the formation of metal hydroxides and precipitates of aluminum and iron. In addition, the treatment produces voluminous gypsum ($CaSO_4$) sludge containing radioactive elements, which presents disposal problems (Falayi, 2014). To be rendered fit for human consumption and other domestic purposes, acidic mineral effluents would have to undergo further treatments, including turbidity removal and disinfection. Aluminum sulfate (alum) is commonly used as a primary coagulant/flocculent in most conventional water treatment plants (WTPs) to remove turbidity, but it has its demerits. It may lead to high aluminum residual content in treated water, which has been shown to promote diseases like Alzheimer's disease [Kaser et al., 1990]. Its use also results in the production of voluminous sludge, adding to the disposal challenges. Chlorination, on the other hand, is the most widely used method for disinfection. However, chlorine has been linked to the potential

formation of carcinogenic and mutagenic disinfection by-products (DBPs) related to increased risks of cancers, heart diseases, and birth defects. Chlorine also suffers from decay, reduced concentration down the distribution network (Devarakonda et al., 2010), and production of voluminous sludge, which further contributes to environmental pollution. Combined with the high cost of chemicals, these shortcomings present a considerable water treatment challenge, particularly in developing countries with scarce resources and poor infrastructure.

The application of natural materials derived from plants in water treatment has increased in recent years. However, of all the studied plant materials, MO seeds have shown promising results as a natural coagulant and biosorbent in water treatment with its performance compared to Alum (Ali et al., 2010; Ghebremichael, 2004). The plant is classified under the single genus Moringaceae family, which constitutes trees indigenous in the tropical region but cultivated in other areas, including South Africa (Suleyman et al., 1994). The seed extracts offer several advantages over conventional water treatment and AMD treatment methods, including zero pH effect on water, low cost, wide availability, no potential health problems, and bio-degradable sludge production (Cochrane et al., 2006; Ndabigengesere et al., 1998). In drinking water clarification, the dried seed suspension acts as a natural coagulant (Arora et al., 2013). This is attributed to the presence of a water-soluble cationic coagulant protein which binds the predominantly negatively charged particulate matter that causes turbidity in water (García-Fayos et al., 2010). High levels of turbidity often indicate high levels of pathogens such as bacteria, viruses, and parasites. MO seeds exert antimicrobial activity against many microbes, including bacteria and fungi (Masden et al., 1987). Suleyman et al. (1994) reported turbidity and bacterial load reductions of 80-99.5% and 90-99.9 %, respectively, after 2 hours of Nile water treatment using MO seeds (Suleyman et al., 1994). Similar findings were reported in later studies by Mohan et al. (2008), Bukar et al. (2010), and Walter et al. (2011). The active antimicrobial agent acts by coagulating the solid matter in water combining it with suspended bacteria for easy removal, hence removing them in the process (Jahn, 1988).

The biosorbent property of moringa seeds qualifies them as a suitable, cost-effective biosorbent alternative for heavy metal remediation in acidic mineral effluents. The biosorption process may be facilitated by the interaction of metal ions(Me^{2+}) with the carboxyl ligands of amino acids present in MO seeds (Kumara et al., 2005). Most of these amino acids exhibit isoelectric points between pH 4.0–8.0 and exist in an ionized state in this pH range (Delvin, 2002). Thus, indicating that MO-Me^{2+} ion binding could proceed via an ion-exchange mechanism driven by electrostatic attraction between Me^{2+} and negatively charged substrates of amino acids (Sharma et al., 2005). However, the complete biosorption mechanism is still not fully understood. The potential mechanism of biosorption may include one or a combination of ion exchange, adsorption, micro precipitation, complexation, chelation, and coordination (Giri, 2012).

It has been noted that much work has been done on the application of MO as a coagulant/flocculant and antimicrobial agent in the treatment of water. However, its application in the treatment of acidic mineral effluents such as AMD is still limited. Therefore, this study sought to establish the effectiveness of MO seed extracts as an alternative antimicrobial agent and biosorbent in the treatment of acidic mineral effluents for disinfection and heavy metal removal, respectively.

2 Materials And Methods

2.1 Reagents and Chemicals

MO seeds were supplied by Rangex (PTY) LTD and used as a biosorbent and antimicrobial agent in the adsorption and antimicrobial activity experiments, respectively. SAME was prepared to fully represent the concentration range usually found for AMD in Witwatersrand, South Africa. The chemicals $CuSO_4$. $5H_2O$, $NiSO_4.7H_2O$, $FeSO_4.5H_2O$ and $MnSO_4.5H_20$ were supplied by C.C. Imelmann (PTY) LTD. Appropriate dilutions of 1000 ppm standard solutions of Ni, Cu, Fe and Mn were prepared for Atomic Absorption Spectroscopy (AAS) calibration. HNO_3 and HCl were used for AAS sample digestion and preservation. 0.1 M HCl and 0.1 M NaOH were used for pH adjustment.

2.2 Characterisation of MO Seeds

The structural elucidation of MO seeds was determined using FTIR (Thermo scientific Nicket (IS10) employing DTGS KBR detector and KBR beam splitter. The spectra were obtained over a range of 800–4000cm^{-1} with a resolution of 2 cm^{-1} and optical velocity of 0.6329. XRF (Rigaku ZSX Primus 11) was used to establish the seed chemical composition. The X-ray source was set at High-Frequency Inverter type with a maximum rating of 4kW, 60kV- 150mA, whereas the primary beam filter and diaphragm were operated at four Filters (Al, Al-2, Cu, Zr) and six-position Automatic Exchanger modes, respectively.

2.3 Adsorption experiments

2.3.1 Sample preparation

SAME constituting of 20 ppm Ni, 20 ppm Cu, 100 ppm Mn and 500 pm Fe was prepared in a 2000 ml volumetric flask by adding appropriate amounts of metal sulphate salts and diluting to volume with reverse osmosis water (RO). This served as the SAME stock solution with an initial pH of 3.36. MO seed kernels were ground to fine powder and dried in the oven at 313 K for 24 hours using the mortar and pestle. This constituted the stock seed extract.

2.3.2 Sample pre-treatment (AAS Analysis)

Before AAS analysis, sample digestion was carried out on treated samples to eliminate organic content and convert target metals into soluble. The procedure involved measuring and transferring 50 ml of filtered (treated) sample into a 100 ml volumetric flask, followed by acidification with 2 ml of 1:1(v/v) HNO_3: H_2O and 1 ml of 1:1(v/v) HCl: H_2O. The sample was then heated on a hot plate and allowed to evaporate to a residual volume of ≈ 20 ml. After cooling, 20 ml was transferred into a 25 ml volumetric flask and diluted to volume with RO water. The sample was then ready for AAS analysis.

2.3.3 Effect of solid loading, pH, temperature, and time

The effect of solid loading was investigated to determine the optimum MO dosage required to achieve the highest metal removal efficiency from SAME. Appropriate amounts (g) of milled MO seeds were

added to 50 ml of SAME in separate 250 ml Erlenmeyer flasks to make sample solutions of 2%, 4%, 6%, 8%, and 10% solid loading. After measuring initial pH, the acidic mineral solution was agitated for 4 h at 150 rpm in a Labotec Orbishaker, thermostatic shaker maintained at 298K, to initiate the adsorption/biosorption process. Samples were taken at intervals of 30mins, filtered using a vacuum filter pump, and pH measurements were done on the filtrate. This was followed by sample digestion (2.3.2), after which samples were stored ready for AAS analysis. The procedure was repeated for the other investigations, each time using optimum conditions obtained in the preceding experiments; pH (2, 3, 4, 5, 6, 7), temperature(298, 308, 318K), and time(0-240 mins). All experiments were done in triplicate to ensure accuracy.

2.3.4 Re-use of spent (metal-loaded) MO seeds.

Milled MO seeds residue cake obtained after filtration in the adsorption experiments was dried for 12 h in an oven set at 323.11 K. The dry spent MO seed cake was then ground to a fine powder using a mortar and pestle. Solid loading, pH, time, and temperature were adjusted to optimum conditions and adsorption process initiated as described in 2.3.3. The procedure was repeated two more times, using loaded MO seed residual cake obtained from the preceding experiment.

2.3.5 Desorption of spent MO seeds

1. 2.5 g of spent MO seeds were added to 100 ml of 0.05 M HNO_3 and subjected to adsorption for 2 h as described in 2.3.3. This was followed by AAS analysis.
2. **2.4 Antimicrobial activity experiments**

2.4.1 MO seed extracts

The MO stock seed extract prepared in 2.3.1 was used to form the raw extract, while the other portion was used to prepare the aqueous extract. To prepare the latter, a portion of the raw seed extract was defatted in 5 % (w/v) n-hexane suspension and stirred with a magnetic stirrer for 60 min. This was followed by centrifuging at 3000 rpm for 45 min to separate the supernatant while the settled powder was allowed to dry at room temperature for 24 h. The defatted dry powder was then mixed with RO water, stirred for 60 min, and allowed to settle for a further 20 min. This was followed by filtration, after which the filtrate was stored as the aqueous extract stock solution ready for antimicrobial experiments.

2.4.2 Antimicrobial Activity

The effect of MO seeds as an antimicrobial agent was determined by investigating the reduction in total microbial load of the synthetic wastewater samples after separate treatments with MO raw extract and aqueous extract at MO dosages of 50 mg/l, 100 mg/l and 150 mg/l. The Quanti-tray and SimPlate procedures as outlined in the ‘Standard Methods for the Examination of Water and Wastewater’ guidelines were used.

2.4.3 Effect of MO seed extracts on coliforms

The Quanti-Tray* Enumeration Procedure was performed. The main objective was to either detect E. coli and total coliforms simultaneously or fecal coliforms in water. *E. coli, Klebsiela and Pseudomonas* were used as control microbes in this study. The results were presented as Most Probable Number (MPN/100 ml), which gives an indication of the most probable number of total bacteria in water samples.

2.4.4 Effect of MO seed extracts on heterotrophic plate count (HPC)

The simPlate procedure was used. The method gives the quantity of HPC (bacteria, yeast, moulds) in water indirectly by testing for the presence of critical enzymes found in these organisms. The results are presented as MPN/100 ml.

3 Results And Discussion

3.1 Adsorption process

3.1.1 Effect of Solid Loading

Figure 1 shows that removal efficiency increases by 2.96%, 4.94%, and 7.29 % for Mn, Ni, and Cu at 10% m/v, respectively, thus making it the optimum solid loading achieved. The Single Factor ANOVA analysis applied at 8–10% (wt/v) solid loading (Table S1- S1.2) proved the increase to be statistically significant at the 5% significance level, with n = 3 for only Ni and Cu. Therefore, solid loading influences Ni and Cu removal from acidic mineral waters. The observed improvement in metal removal efficiency could be due to increased surface area, leading to more available active sites and a subsequent higher degree of adsorption. Metal removal followed the order; Ni > Cu > Fe > Mn. The physicochemical properties of metal ions are presented in Table 1 and could be responsible for the observed removal trend.

Table 1
Physicochemical properties of metal ions

(source: Bhatt, 2015; Pauling scale-periodic table)

Metal ion	Ionic radius	Electronegativity	Electron configuration	Para magnetism
Ni^{2+}	0.55	1.91	$(Ar)3d^{8}4S$	weakly
Cu^{2+}	0.57	1.90	$(Ar)3d^{9}4S$	weakly
Fe^{2+}	0.63	1.83	$(Ar)3d^{6}4S$	Highly
Mn^{2+}	0.66	1.55	$(Ar)3d^{5}4S$	Highly

Table 1 shows a decrease in the ionic radius following the order: Mn > Fe > Cu > Ni, which resonated with the observed increase in removal efficiency. To explain this, it was considered that the smaller the metal ion, the closer it can get to the active site and the tighter it can be bound. Hence there would be a stronger

attraction for it than larger metal ions. On the other hand, a decrease in electronegativity followed an opposite trend: Ni > Cu > Fe > Mn. However, higher electronegativity results in enhanced adsorption tendency of Me^{2+} (Gorgievskia et al., 2013; Zhang 2011), which is consistent with the findings of this study. Therefore, the smaller the ionic radius, the larger the electronegativity and the higher the affinity of Me^{2+} ions for active sites.

3.1.2 Effect of pH

Fig.2 Variation of metal removal with initial pH. [Conditions: C_o = 20 ppm Cu, 20 ppm, Ni, 100 ppm Mn, 500 ppm Fe; solid loading = 10% m/v, Temperature = 298 K

Metal removal increases of 69.6%, 68.6, 57.0%, and 22.4% were achieved for Cu, Ni, Fe, and Mn, respectively, from pH 2 to pH 3 (Fig. 2). The increase was proven to be statistically significant at the 5% significance level with n = 3, for all the metals using the ANOVA analysis (Table S1.3-S1.6) at pH 2–3. Thus, metal removal for Ni, Cu, Fe, and Mn was primarily influenced by pH, and pH 3 was the optimum pH achieved. Metal removal remained relatively constant with a further increase in pH up to 7, thus indicating sorption equilibrium. The rise in metal removal from pH 2 to 3 could be attributed to metal ions (Me^{2+}) competing more favourably than H^+/H_3O^+ ions for biosorbent active sites (since H^+ concentration is lower). Thus, resulting in higher metal uptake and consequently higher removal efficiency and vice-versa for pH < 3.

Furthermore, at pH < 3, the adsorbent surface area is positively charged, hence exhibits negligible affinity for Me^{2+} ions (Farooq et al., 2010). Figure 2 further shows that Mn removal was very poor, which could be attributed to its lower affinity for active binding sites due to its lower electronegativity and higher ionic radius. However, at a pH range of 6–7, a 49.9% increase in Mn removal was achieved. Mn (II) could have possibly been oxidized to Mn(III/IV) during pH adjustments using NaOH and therefore precipitated as MnO_x (Pinto and Al-Abedb 2011) at this pH range. Therefore Mn removal was probably via precipitation mechanism to a more significant extent. Traditionally, Mn removal from acidic mineral waters is low (Deepti et al., 2016)

3.1.3 Effect of contact time

Metal removal efficiency increased with time reaching maximum levels of 90.0%, 81.2%, and 69.2% for Ni, Cu, and Fe, respectively, at 90min residence time (Fig. 3). The ANOVA analysis applied at 30–90 mins showed a statistical significance in Ni, Cu, and Fe removal at the 5% significance level with n = 3 (S1.7-S1-9). Therefore, removal efficiency for Ni, Cu, and Fe was due to an increase of residence time from 30–90 mins, with 90 mins being the optimum residence time achieved. A decline then followed this in Cu removal while static levels were achieved for Ni and Fe at sorption equilibrium. The initial increase in metal removal may be ascribed to the sizeable biosorbent contact surface area available at the start of the biosorption process as many active binding sites are still unoccupied. However, as adsorption proceeds, the number of available active sites diminishes, and the biosorption rate slows down until sorption equilibrium is reached. At this stage, Me^{2+} ions compete significantly for the few remaining

active sites. The mechanism responsible for the rapid metal removal phase could be physical adsorption or ion exchange at the surface of biosorbent, while the slower phase could be due to other mechanisms such as aggregation, micro-precipitation, and saturation of binding sites (Pinto and Al-Abedb 2011).

3.1.4 Effect of temperature

Figure 4 shows that from 298 K to 308 K, there was an increase of 28.5%, 20.7%, 36.0%, and 7.7% removal efficiency for Ni, Cu, Fe, and Mn. The increase in metal removal was proven by ANOVA analysis at 298 K- 308 K (Table S1.10-S1.13) to be statistically significant for Mn at a 5% significance level. Thus, metal removal was dependent on temperature. The optimum temperature achieved was 308 K. Further temperature increases to 318 K resulted in a decline in removal efficiency, which was more pronounced for Mn and Fe at 33.2% and 12.3% respectively.

The enhancement of metal removal with increasing temperature demonstrated the endothermic nature of the biosorption process. Increasing temperature led to increased kinetic energy and surface activity of metal ions. Thus, promoting additional metal binding capacity. Furthermore, the observed increase in metal removal with temperature could be ascribed to the decreased boundary layer thickness surrounding the biosorbent. The net effect reduces the mass transfer resistance of Me^{2+} ions in the boundary layer (Reddy et al., 2010). On the other hand, the decrease in metal removal observed at 318K was most probably due to the damage done to the physical structure of the bio sorbent resulting in loss of adsorption capacity. Structure highly defines protein functionality, thus at high temperatures, the tertiary structure and therefore functionality of the Moringa bioactive functional groups are destroyed since they are proteinaceous in nature.

3.2 Biosorption thermodynamics

Table 2
Thermodynamic parameters influencing adsorption process.

Metal ion	**Metal**	**ΔH∘**	**ΔS∘**	**ΔG∘**
Temperature/K		**(KJ/mol)**	**(KJ/mol)**	**(KJ/mol)**
				298 308 318
	Ni	149.2	44.9	0.337 -0.783 -2.647
	Cu	142.7	42.5	-0.080 -1.390 -2.927
	Fe	81.2	27.7	4.031 1.702 2.407
	Mn	5.1	5.8	4.244 4.238 4.144

Figure 5 shows that ΔG∘ varies inversely with temperature. As shown in Table 2, ΔG° values were negative for Cu and Ni, suggesting that the process was feasible and spontaneous for these two metals. The increase in ΔG° values with temperature, on a negative scale for Cu and Ni (Table 2), shows larger spontaneity at higher temperatures, thus implying an increased probability of the sorption process. For Fe

and Mn, the biosorption process is thermodynamically non-spontaneous, as indicated by the positive ΔG° values across all the temperature values used herein (Table 2). ΔH° values are positive for all metals signifying the endothermic nature of the adsorption process. ΔS° values were positive, indicating an increase in the degrees of freedom on the surface of the sorbent and disorder of the system. This must have been accompanied by a considerable change in surface configuration of the bio sorbent due to strong metal affinity for the bio sorbent. Furthermore, the positive ΔS° values may also indicate that ion exchange occurs and brings about steric hindrances (Lyubchik et al., 2012). Thus, for the adsorption reaction to proceed spontaneously, ΔG°< 0, ΔS° > 0 and ΔH° > 0.

3.3 Adsorption isotherms

3.5.1 Langmuir and Freundlich isotherms

Table 3
Equilibrium parameters evaluated from the Langmuir and Freundlich isotherms (S1).

Metal	Langmuir			Freundlich	
	RL(dm^3/g)	qm(mg/g)	b(L/g) R^2	K_f	n R^2
Cu	0.06	0.11	0.74 0.99	43.91	0.35 0.99
Ni	0.04	0.12	1.33 0.99	4444.53	0.25 0.99
Fe	0.15	1.47	0.10 0.99	754.57	0.78 0.99
Mn	0.44	0.01	0.01 0.80	66.67	8.46 0.94

Table 3 shows that the experimental data for Cu, Ni, and Fe could be well represented by the Langmuir and Freundlich models as indicated by the R^2 values of 0.99. R_L values lie in the range $0 < R_L \leq 1$, showing the suitability of Moringa seeds as a bio sorbent for the adsorption process. The affinity of Moringa seeds for the metal ions followed the order Ni > Cu > Fe > Mn as shown by the corresponding 'b' values of 1.33, 0.74, 0.10, and 0.01, respectively. High 'b' values reflect the high affinity of the bio sorbent for the metal. A similar trend was obtained for the adsorption capacity (q_m) except for Fe, which showed an anomaly with the highest value of 1,47mg/g. This could have been due to steric hindrance effects of the larger Fe^{2+} ion on the adsorption of smaller Cu^{2+} and Ni^{2+} ions. Furthermore, being highly paramagnetic, Fe is more strongly attracted by the magnetic field (probably originating from the biosorbent) than the weakly paramagnetic Ni and Cu. (Table 1)

3.4 Temkin and Dubinin- Radushkevich models

Table 4
Temkin and Dubinin- Radushkevich parameters

Metal Cu Ni Fe Mn
Temkin
B(J/mol) 19.44 16.53 0.80 0.52
AT(L/g) 1.21 1.21 700.32 47.73
R2 0.97 0.91 0.99 0.99
Dubinin-Radushkevich
KDR(mol12/KJ2) 0.01 18.85 1.58 571.91
Qm(mg/g) 6.28 4.38 4.09 8.46
R2 0.87 0.66 0.83 0.83
Es(J/mol) 13.61 0.23 0.80 0.04

Table 4 shows that the adsorption process is best described by the Temkin model. The low A_T and B values signify the ionic exchange nature of the adsorption process.

3.5 Adsorption Kinetics

Table 5
Adsorption Kinetics Parameters

Pseudo First Order			Psedo 2nd order			
K_1	qe_1	R^2	K_2	qe_{calc}	qe_{exp}	R^2
Ni 0.028	139.12	0.994	0.25	0.214	0.186	0.995
Cu 0.003	16.177	0.397	0.748	0.164	0.150	0.977
Fe 0.021	1.561	0.096	0.030	5.063	3.469	0.886
Mn 0.016	14.49	0.351	0.008	0.372	0.217	0.476

Table 5 shows that the 2nd order model best describes the adsorption kinetics of Ni and Cu, thus implying a chemisorption mechanism consistent with monolayer adsorption. qe_{calc} is in strong agreement with qe_{expt} for these two metals, thus further confirming the suitability of the pseudo 2nd order model in describing the adsorption process. However, the model was insufficient to represent the experimental data for Fe and Mn.

3.6 Re- use of Moringa Seeds as a bio-sorbent Fig.6 Variation of metal removal with the number of recycles of MO seed extract.

From the second to the third cycle, metal removal efficiency decreased from 63–39%, 47–27%, 55–11%, and 19–13% for Ni, Cu, Fe, and Mn, respectively (Fig. 6). Thus, implying that the seeds extract can be effectively re-used for metal removal for two cycles. The observed trend could be attributed to the fewer remaining active sites for metal binding after each cycle.

3.7 Desorption studies

Table 6
percentage amount of metal recovered from metal loaded milled MO seeds.

Concentration/mg Metal Original After agitation leached from MLSE	Adsorbed from SAME	% leached from MLSE
Ni 0.17 13.97 13.80	18.62	74.09
Cu 0.11 9.37 9.26	15.06	61.50
Fe 0 173.32 173.32	366.26	47.32
Mn 0 17.06 17.06	31.66	53.88

The solution of 0.05 M HNO_3 was able to leach all metal ions from metal-loaded MO seeds extract except for Fe, which had below 50% leaching efficiency (Table 6). This indicates the possibility of recycling spent MO seeds extract for further metal removal in acidic mineral waters.

3.8 Antimicrobial Activity

3.8.1 Effect of MO seed extract on coliforms

Total coliform inhibition seemed to increase with MO dosage reaching a maximum of 100% for the aqueous extract and 98.2% for the crude extract at 150mg/l MO dosage, as shown in Fig. 7. The increase was proven by ANOVA (Table S2) to be statistically significant at the 5% significance level, with n = 3, with the difference in dosages being the most probable factor.

3.8.2 Effect of MO seed extracts on HPC

HPC load reduction increases with increasing MO dosage, reaching maximum reductions of 90.5% and 86.1% at 150mg/l MO dosage for the crude extract and raw extract, respectively (Fig. 8). The increase is statistically significant at the 5% significance level and is probably influenced by the difference in the seed extracts used (Table S2). The findings depicted in Fig. 7 and Fig. 8 agree with those of authors such as Atieno et al. (2011), Mangale et al. (2012) and Amagloh, and Benang (2009. The observed bacterial load reductions could be due to antimicrobial properties of the bioactive agent, 4 -alpha rhamnosyloxybenzyl isothiocyanate (Masden et al., 1987), which is presumed to act by disrupting the cell membrane causing leakage of cytoplasmic content and killing the bacterial cell (Walter et al., 2011; Arora et al., 2013). Furthermore, Munyanziza and Yongabi (2007) reported that the aqueous extract contains

higher levels of pterygospermin, an antibiotic agent which destroys microorganisms in water. The increase in total bacterial load reduction with MO dosage could be due to more bioactive agents available to interact with the bacteria at higher MO dosages. The enhanced effectiveness shown by the aqueous extract could be explained by considering that the aqueous extract constitutes mainly of the protein component of the seeds, thus implying a higher concentration of the bioactive agent and consequently higher antimicrobial activity than the raw extract.

These findings are encouraging since they meet the EPA drinking water standards which stipulate zero levels for total coliforms and E.coli in drinking water. The presence of coliforms is an indirect indication of dangerous pathogens in drinking water, thus implying adverse health risks on humans.

3.9 Chemical composition of MO seeds

Table 7
XRF analysis of raw and loaded MO seeds

Constituent	Raw	
	MO	loaded MO
MgO	0.334	0.178
Al_2O_3	0.0472	0.0512
SiO_2	0.111	0.115
P_2O_5	1.41	1.64
SO_3	4.05	1.68
Cl	0.0404	0.0344
K_2O	0.782	0.226
CaO	0.193	0.148
MnO	0.00270	0.0903
Fe_2O_3	0.0132	0.714
NiO	0.00140	0.0152
CuO	0	0.0214
ZnO	0.00490	0.00610
SrO	0.000700	0.000800
BaO	0.0279	0
C	93.0	95.1

Table 7 shows that C is the principal constituent of the MO seeds. After metal-loading, the proportions of Ni^{2+}, Cu^{2+}, $Fe^{2+,}$ and Mn^{2+} increased, probably due to the biosorption of these metals onto active MO binding surfaces. The ratios of Ca^{2+}, Mg^{2+}, $K^{2+,}$ and Ba^{2+} decreased as these were most likely involved in the ion-exchange mechanism of adsorption and were therefore exchanged with metal ions in the active binding sites (Gupta et al., 2013).

3.10 MO seed characterisation

Figure 9 (a) shows the FTIR spectrum for MO seeds before metal loading. The spectrum exhibits a broad peak at 3284.30 cm^{-1} due to the stretching vibration of phenolic hydroxyl group –OH (Packialakshmi et al., 2014). The –OH group represents hydrogen bonding and has been predominant in the protein and fatty acid structures of the MO seeds (Vanessa et al., 2013). The -C-H stretching of –C = O and/ $-CH_3$ functional groups could have contributed to the absorption peaks observed at 2919.49 cm^{-1} and 2847.49 cm^{-1} while the sharp and elongated peak at 1650.34 cm^{-1} could be assigned to -C = C stretch or –C = O group of carboxylic acids (Nyoni et al., 2017). The peak at 1538.06 cm^{-1} could be associated with -C-N stretching and -N-H deformation in the peptide ($-CONH_2$) group linking the seed proteins (Araújo et al., 2010). Symmetric bending of CH_3 may have occurred at peak 1414.9670 $cm^{-1,}$ while the stretching vibration of –C = O in the ester group could be represented by the peak 1231.7070cm^{-1}. Peak 1052.6470cm^{-1} probably correspond to -O-H stretching of polysaccharides, whereas the presence of weak peaks at 925.5970 cm^{-1} and 792.0770 cm^{-1} indicates possible out-of-plane bend an ester ($-O-CH_3$ and alkene (–C = C-) group respectively.

Figure 9 (b) presents the FTIR spectrum of MO seeds after the biosorption process. Some shifts in the peaks were noted; peak 3284,30cm^{-1} shifted to 3293.70 cm^{-1}, 2919.49 shifted to 2925.17 cm^{-1}, 2847.50 cm^{-1} to 2857.00 cm^{-1}, 925.60 cm^{-1} to 871.78 cm^{-1} and 792.08 cm^{-1} to 789.72 cm^{-1}. These shifts were probably caused by the –C = O stretching (Ali et al., 2015), which can be linked to esters, saturated aliphatic groups, and α,β-unsaturated aldehydes, and ketones (Rahim et al., 2014) owing to the heterogeneous nature of the MO seeds. The lipid component of the seeds is represented by the carbonyl amides in the protein portion, which may be responsible for the shoulder peak at 1736.95 cm^{-1} (Vanessa et al., 2012). The resultant repeated shift of the -C = O stretching implies that the -C = O group could be responsible for binding/reacting with Me^{2+} ions at the surface of the MO seeds. The presence of peaks 2925.16 confirms the protein structure of MO seeds and 2856.99 cm^{-1}, which may be respectively assigned to symmetrical and asymmetrical C—H stretching of the $-CH_2$ moiety in fatty acids (Vanessa et al., 2012). The evolution of new peaks at 234470.06 cm^{-1} and 1736.96 cm^{-1} suggests a change in the natural composition of MO seeds due to the biosorption process.

Conclusion

Conclusion

The MO seed extract demonstrated that they could be used as effective biosorbent material for the removal of Ni, Cu, and Fe in acidic mineral effluents. Mn removal was very poor, probably due to its low affinity for the MO biosorbent. The Langmuir model and second-order kinetics best described the adsorption process for Ni, Cu, and Fe, with ion exchange and/chemisorption being the potential mechanisms of adsorption. The adsorption process for all metal ions was endothermic but only thermodynamically feasible for Ni and Cu. Metal removal followed the order: Ni > Cu > Fe > Mn, with ionic radius and electronegativity being the major influencing factors. Metal removal efficiency increased with pH, time, % solid loading, and temperature till the attainment of sorption equilibrium. Optimum operating conditions achieved were pH = 3, Temperature = 308K, % solid loading = 10%, and residence time of 90 minutes. Metal removal in the second cycle of the desorption treatment was quite low, thus indicating that spent seed extract could be effectively recycled for only two cycles. The seeds also seem to exhibit high antimicrobial activity as indicated by the 100% total bacterial load reduction and inhibition on *E.Coli* and HPC. However, at 150mg/l MO dosage, the aqueous extract proved to be more effective than the raw extract achieving maximum reductions of 100% and 90.5% in coliform and HPC inhibition, respectively. Thus, it is recommended to use the raw extract as an antimicrobial agent in the treatment of acidic mineral effluents.

Overall, the research findings indicate that MO seed extracts could be effectively used as alternative antimicrobial agents and biosorbent in treating acidic mineral effluents for disinfection and heavy metal removal, respectively. Thus, providing an alternative AMD treatment method that is cost-effective, easily accessible, environmentally friendly (forms bio-degradable sludge), and poses no potential health risks, particularly on humans

Declarations

Funding

Not applicable

The authors have no relevant financial or non-financial interests to disclose.

Conflicts of interest/Competing interests.

The authors declare no conflict/competing interests.

Ethics approval and Consent to participate.

Not applicable

Availability of data and material

All data generated or analyzed during this study are included in this published article (and its supplementary information files).

Code availability

Not applicable

Authors' contributions

All authors contributed to the study conception and design. Material preparation, Experiments, data collection and analysis were performed by Pauline Ncube. The first draft of the manuscript was written by Pauline Ncube and proofread by Freeman Ntuli and Thabo Falayi. All authors read and approved the final manuscript.

Consent for publication

The authors give consent to the publication of this manuscript and further declare that this work has not been published before; that it is not under consideration for publication anywhere else and that its publication has been approved by the University of Johannesburg.

Acknowledgments

The authors gratefully acknowledge the research support extended by the Department of Chemical Engineering, University of Johannesburg.

References

1. Ali EN, Alfarra SR, Yusoff MM, Rahman MdL (2015) Environmentally Friendly Bio sorbent from Moringa Oleifera Leaves for Water Treatment. *International Journal of Environmental Science and Development 6, 101–105.*
2. Ali NA, Muyibi SA, Salleh HM, Zahangir MD (2010) “Production of Natural Coagulant from Moringa Oleifera Seed for Application in Treatment of Low Turbidity Water.” *Journal of Water Resource and Protection 2, 259–266.*
3. Amagloh FK, Benang A (2009) Effectiveness of Moringa Oleifera Seeds as a Coagulant for Water Purification. Afr J Agric Res 4:119–123
4. Araújo CST, Carvalho D, Rezende H, Almeida C, Coelho LL,S, Coelho L,M, Marques NM,M, Alves TL, V, N., 2013. Bioremediation of Waters Contaminated with Heavy Metals Using Moringa Oleifera Seeds as Biosorbent. *Journal of the Brazilian Chemical Society 21, 1727–1732.*
5. Arora DS, Onsare JG, Kaur H (2013) Bioprospecting of Moringa (Moringaceae): Microbiological Perspective. Journal of Pharmacognosy Phytochemistry 1:193
6. Atieno W, Wagai S, Arama S, Ogur P, J., 2011. Antibacterial Activity of Moringa Oleifera and Moringa Stenopetala Methanol and n-hexane Seed Extracts on Bacteria Implicated in Water Borne Diseases. *African Journal of Microbiology Research 5, 153–157*
7. Bhatt V (2015) Essentials of coordination chemistry. United Kingdom, Academic press publisher

8. Bukar A, Ubar A, Oyeyi TI (2010) Antimicrobial Profile of Moringa Oleifera Lam extracts against some Food- borne microorganisms. *Bayero Journal of Pure and Apllied Science 3, 43–48*
9. Cochrane EL, Lua Sb, Gibb SWa, Villaescusa I (2006) A comparison of low-cost bio-sorbents and commercial sorbents for the removal of copper from aqueous media. J Hazard Mater B137:198–206
10. Deepti SP, Sanjay M,C, John U,K (2016) A review of technologies for Manganese removal from wastewaters. *Journal of Environmental Chemical Engineering 4, 468–487*
11. Delvin S (2002) Amino acids and proteins, 1st edn. IVY publishing house, New Delhi
12. Devarakonda V, Moussa N,A, VanBlaricum V, Ginsberge M, Hock V (2010) Kinetics of free Chlorine decay in Water distribution Networks, Proc. The World Environmental and Water Resources Congress, ASCE, Rhode Island, May 16–20
13. EPA: Environmental Protection Agency. National Primary Drinking Water Regulations. Accessed on 17 (April 2020) from: http://www.biovir.com/Images/pdf054.pdf
14. Expert Team of the Inter-Ministerial Committee (2010) Mine water management in the Witwatersrand Gold Fields with special emphasis on acid mine drainage. In: Report to the Inter-Ministerial Committee on Acid Mine Drainage. Pretoria, Department of Water, Pretoria
15. Falayi T (2014) Adsorption of Heavy Metals and Neutralization of Acid Mine Drainage using Clay Minerals. *Masters Dissertation, University of Johannesburg*
16. Farooq U, Kozinski JA, Khan M, Athar A, M., 2010. Biosorption of Heavy Metal Ions using Wheat based biosorbents – A review of the recent literature. *Bio resource Technology 101, 5043–5053*
17. Garcia-Fayos B, Arnal JM, Verdu G, Sauri A (2010) Study of Moringa Oleifera Oil Extraction and its Influence in Primary Coagulant Activity for Drinking Water Treatment. Paper presented at the *annual meeting for the organisation of CABI, Valencia, 25–29 October.*
18. Ghebremichael KA (2004) Moringa seed and pumice as alternative natural material for drinking water treatment. *PhD thesis, KTH land, and water resources engineering*
19. Giri A (2012) Removal of Arsenic (III) and chromium (VI) from the water using phytoremediation and bioremediation techniques. *Dissertation, National Institute of Technology*
20. Gorgievskia M, Boˇzic´ D, Stankovi'c´ V, ˇStrbac N, ˇSerbulab S (2013) Kinetics, Equilibrium, and Mechanism of Cu2+, Ni2 + and Zn2 + ions biosorption using wheat straw. *Ecological Engineering 58: 113– 122*
21. Gupta VK, Ali I, Saleh TA, Siddiqui MN, Agarwal S (2013) Chromium removal from water by activated carbon developed from waste rubber tires. *Environmental Science and Pollution Research 20, 1261–1268.*
22. Jahn SAA (1988) Using Moringa seeds as coagulants in developing countries. *Journal of American Water Works Association 80, 43–50.*
23. Kaser F, Werner C, Nahayo D (1990) Rural water treatment using Moringa oleifera seeds as coagulant. Natural Resources Development 33:33–47

24. Kumara V, Narayana J, Puttaiah ET, Babu KH (2005) Assessment of surface and sub-surface water of Bhadra river basin near Bhadravathi town Karnataka. *Journal of Ecotoxicology & Environmental Monitoring. 15, 253–261.*
25. Lyubchik SI, Lyubchik A,I, Galushko O, Tikhonova L, Vital L,P, J (2012) Kinetics and Thermodynamics of the Cr(III) Adsorption on the Activated Carbon from Comingled Wastes. Colloidal Surfaces 242:151–158
26. Madsen M, Schlundt J, Omer F,E (1987) Effect of Water Coagulated by Seeds of Moringa Oleifera on Bacterial Concentrations. Journal on Tropical Medical Hygiene 90:101–109
27. Mangale SM, Chonde S, Jadhav G, Raut AS, P, D., 2012. Study of Moringa Oleifera (Drumstick) Seed as a Natural Absorbent and Antimicrobial Agent for River Water Treatment. *Journal of Natural Product and Plant Resource 2, 89–100*
28. Mohan JS, Bipinraj N, Gidde K, M, R., 2008. Moringa Oleifera Seed as Antibacterial Agent in Water Treatment. Paper for National Conference on Household Water Treatment Technology, at Hindustan College of Sc. And Tech. July 24–25
29. Munyanziza E, Yongabi K, A., 2007. Moringa Peregrina (Forssk.) Fiori In: van der Vossen AM and Mkamilo GS, (Editors)., Wageningen, Netherlands, 2007
30. Muyibi S, Evison A, L.M (1994) Moringa Oleifera Seeds for Softening Hardwater. Water Res 29:1099–1105
31. Ndabigengesere A, Subba K, Narasiah M (1998) Quality of Water treated by Coagulation using Moringa oleifera seeds. Water Res 32:781–791
32. Nyoni S, Satiya E, Mukaratirwa-Muchanyereyi N, Shumba M (2017) Comparative biosorption of Pb2 + ions from aqueous solution using Moringa oleifera plant parts: Equilibrium, kinetics, and thermodynamic studies. *African Journal of Biotechnology, 16, 2215–2231.*
33. Packialakshmi N, Naziya S (2014) Fourier transform infrared spectroscopy analysis of various solvent extracts of Caralluma fimbriyata. Asian Journal of Biomedical Pharmaceutical Sciences 4:20
34. Pinto PX, Al-AbedB S, R (2011) Biosorption of Heavy Metals from Mining Influenced Water ontoChitin Products. Chem Eng J 166:1002–1009
35. Rahim M, Vadi M (2014) Langmuir, Freundlich and Temkin Adsorption Isotherms of Propanol on Multi- wall Carbon Nanotube. *Journal of Modern Drug Discovery and Drug Delivery Research 19, 1–3.*
36. Reddy DHK, Ramana DKV, Seshaiah K, Reddy AVR (2010) Biosorption of Ni(II) from Aqueous phase by Moringa Oleifera Bark, a Low Cost Biosorbent. *Desalination 268, 150–157.*
37. Sharma V, Paliwal R (2013) Isolation and Characterization of Saponins from Moringa Oleifera (Moringaeceae) pods. J Pharm Sci 32:406–413
38. Vanessa N, Alves VN, Coelho NMM (2012) Selective extraction and preconcentration of chromium using Moringa oleifera husks as bio sorbent and flame atomic absorption spectrometry. *Microchemical Journal 109, 16–22*

39. Walter A, Samuel W, Peter A, Joseph O (2011) Antibacterial Activity of Moringa Oleifera and Moringa Stenopetala Methanol and n-Hexane seed Extracts on Bacteria implicated in water borne diseases. *African Journal of Microbiology Research 5, 153–157*
40. Zhang M (2011) Adsorption Study of Pb(II), Cu(II) and Zn(II) from Simulated Acid Mine Drainage using Dairy Manure Compost. Chem Eng J 172:361–368

Figures

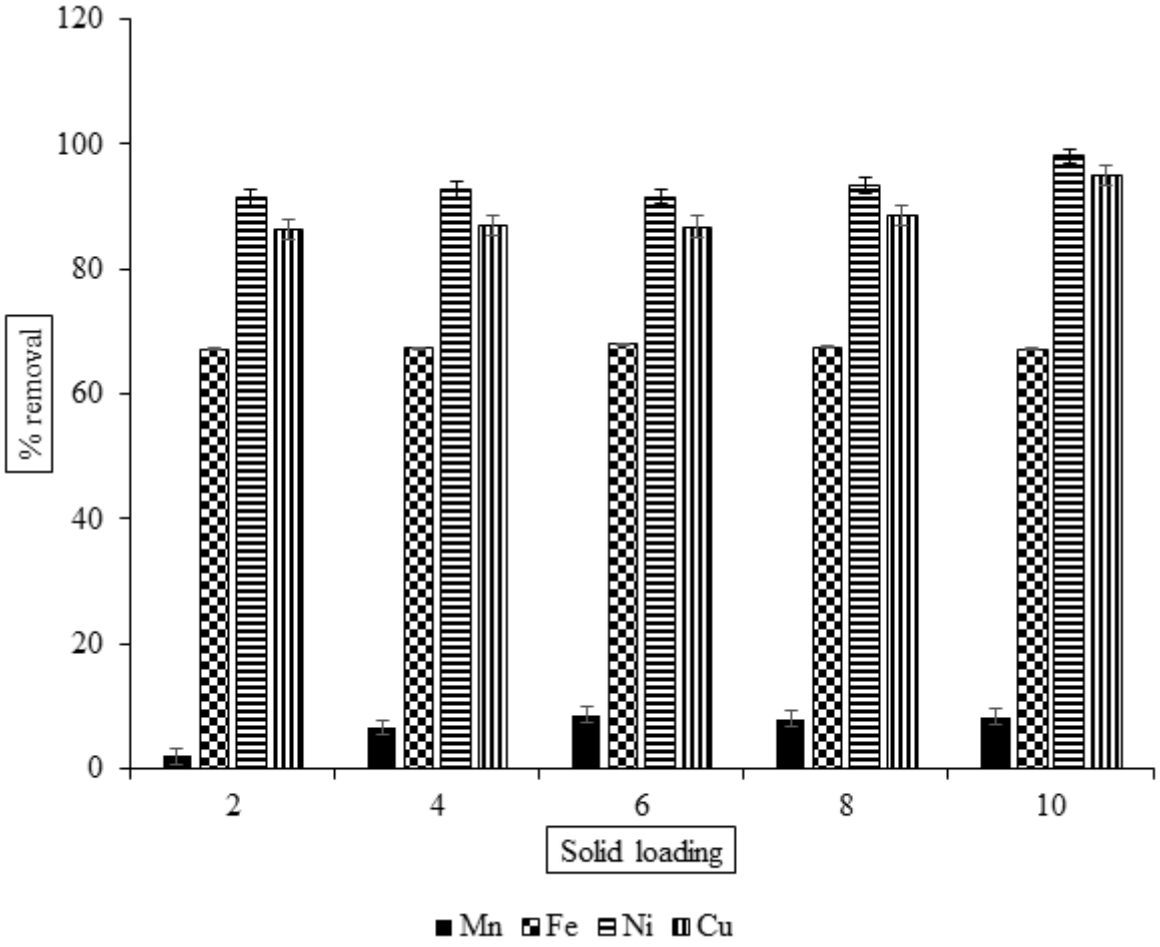

Figure 1

Variation of metal removal with solid loading. [Conditions: Co = 20 ppm Cu, 20 ppm Ni, 100 ppm Mn, 500 ppm Fe, Temperature = 298 K, initial pH =3.4, Time = 4h]

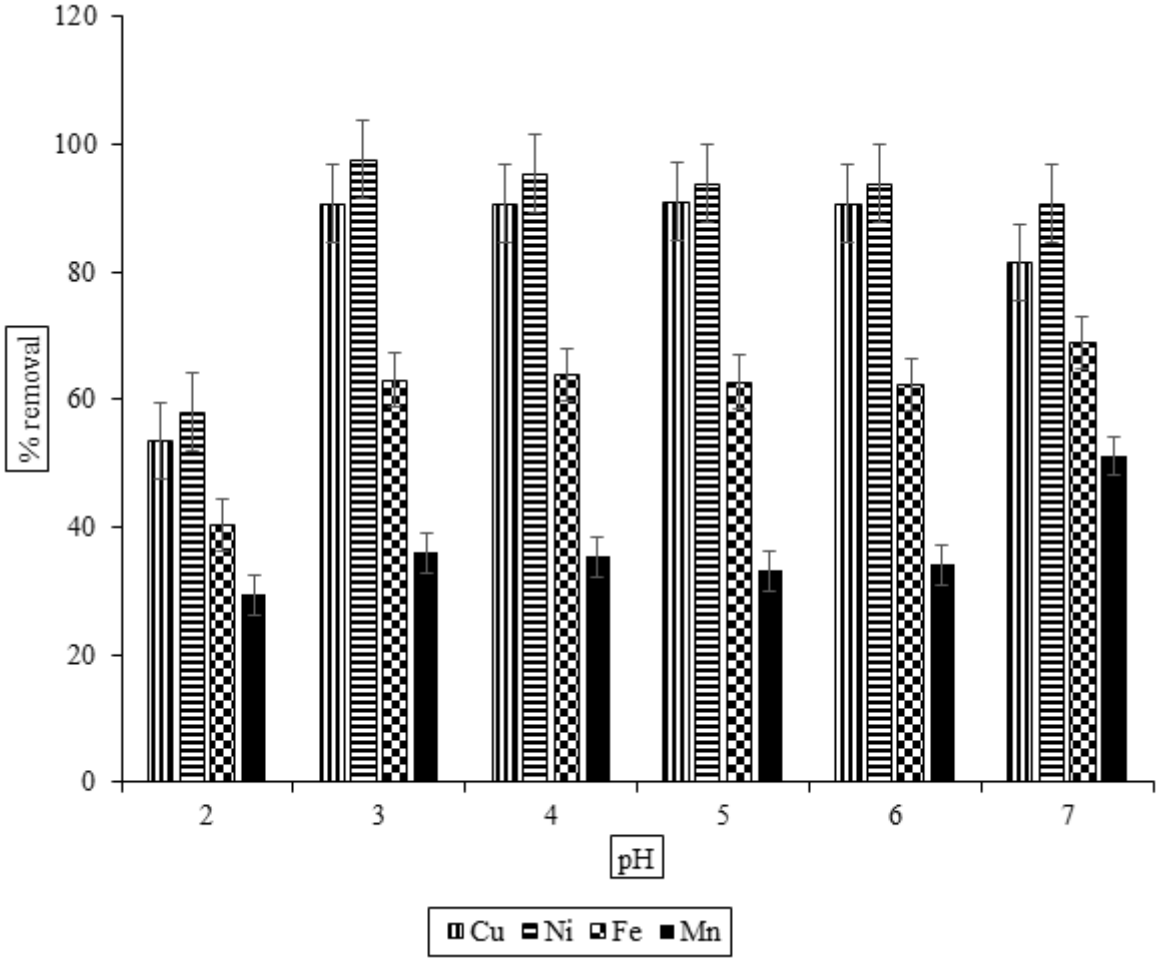

Figure 2

Variation of metal removal with initial pH. [Conditions: Co = 20 ppm Cu, 20 ppm, Ni, 100 ppm Mn, 500 ppm Fe; solid loading = 10% m/v, Temperature = 298 K

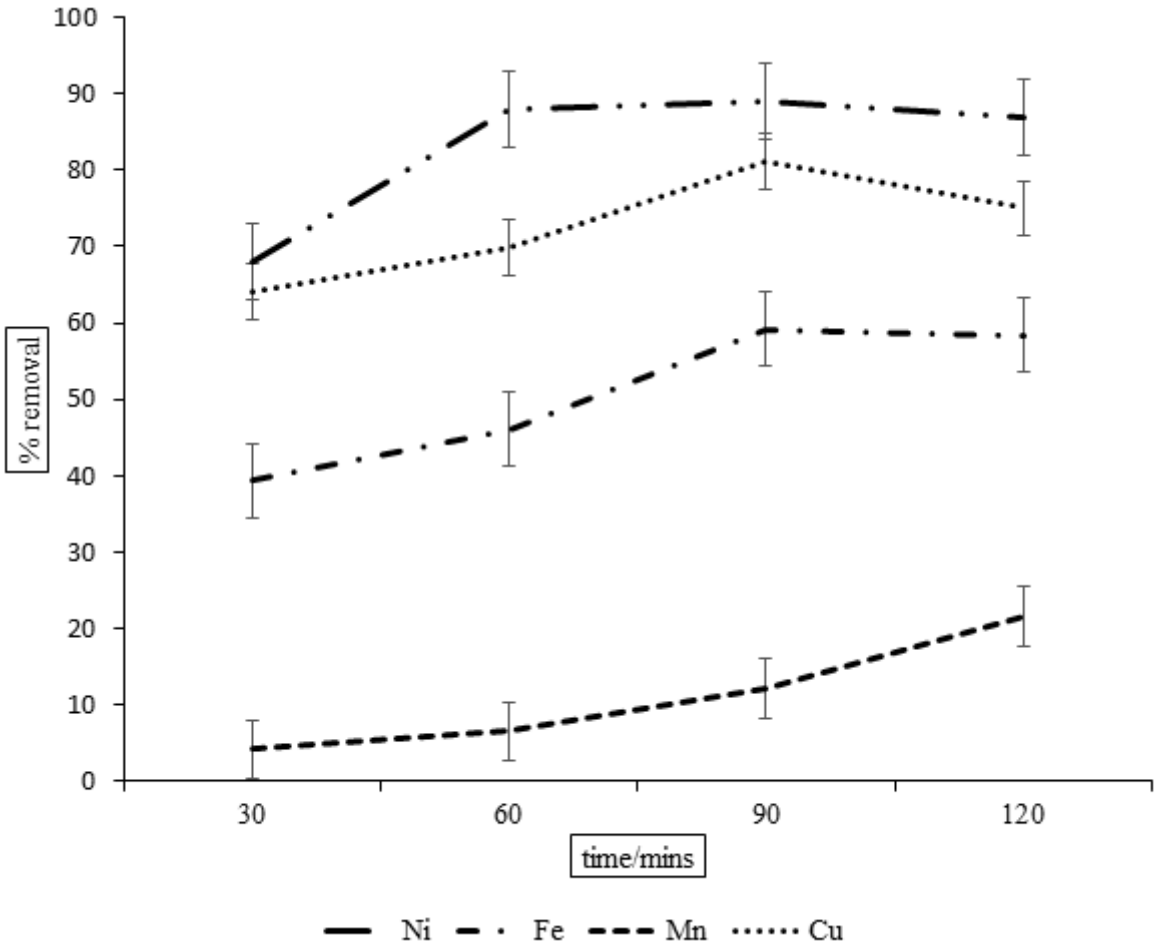

Figure 3

Variation of metal removal with contact time. [Conditions: Co = 20 ppm Ni, 20 ppm Cu, 100 ppm Mn, 500 ppm Fe; solid loading = 10% m/v, initial pH = 3, temperature = 298 K]

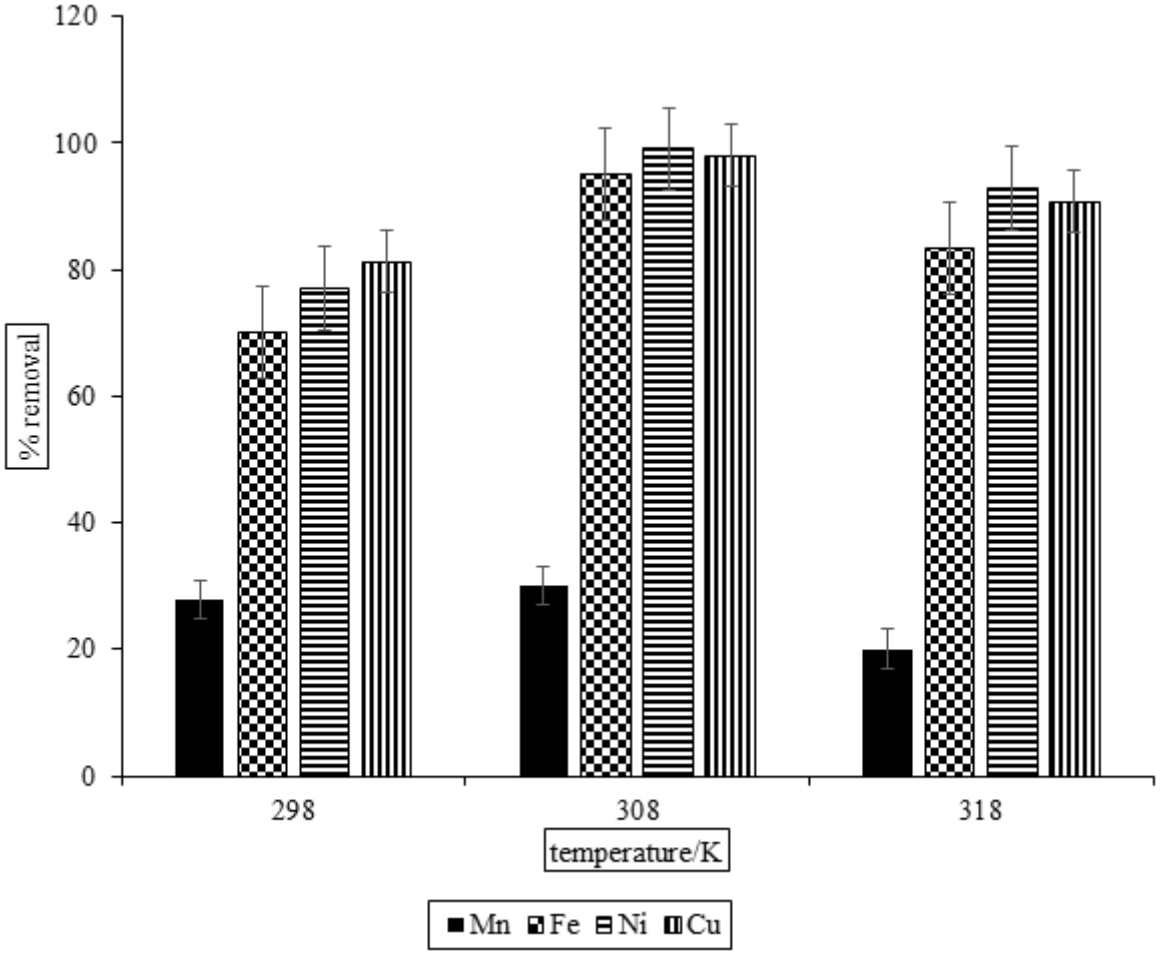

Figure 4

Variation of metal removal with temperature [Conditions: Co: 20 ppm Cu, 20 ppm Ni, 100 ppm Mn, 500 ppm Fe, initial pH =3.0, solid loading = 10% m/v, time = 90 mins]

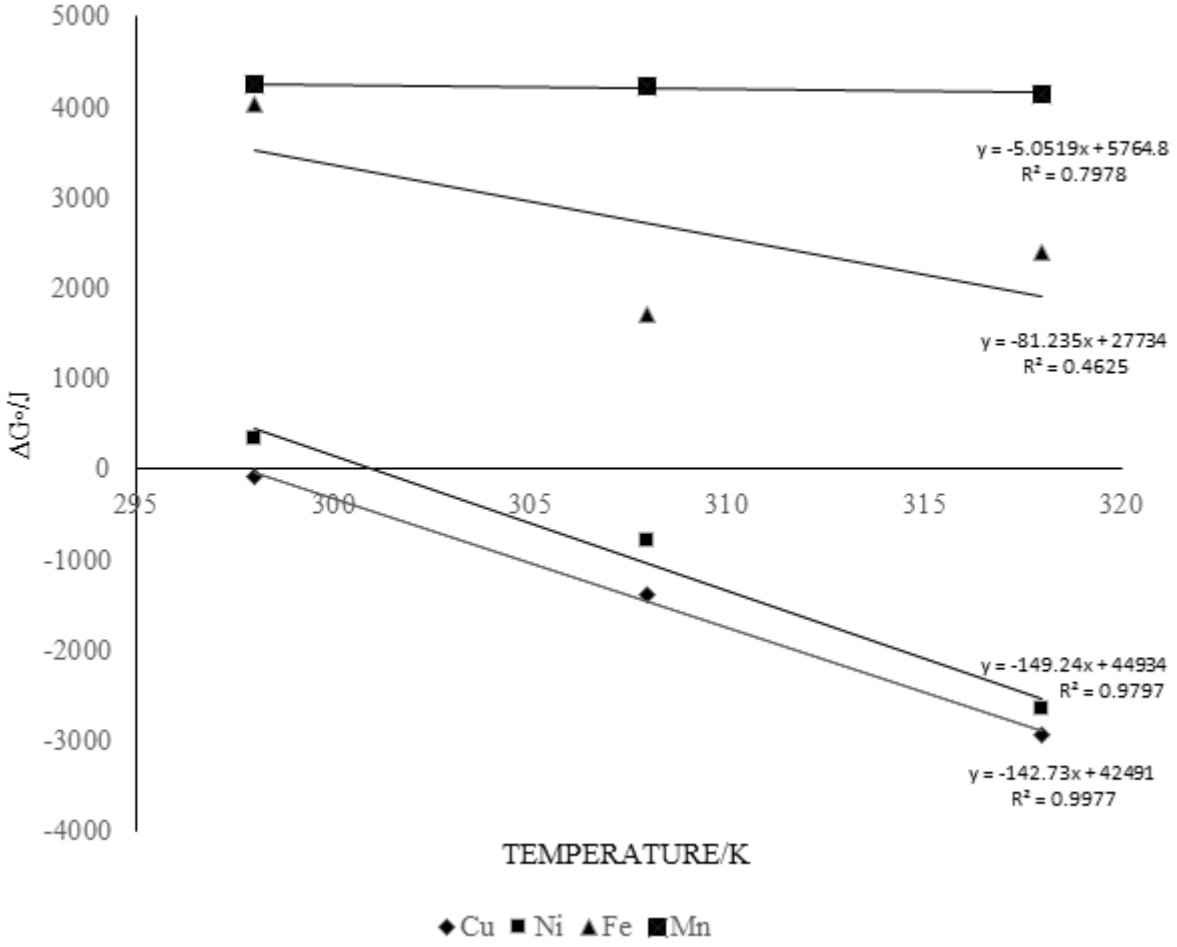

Figure 5

ΔG∘ vs T plot for Cu, Ni, Fe and Mn

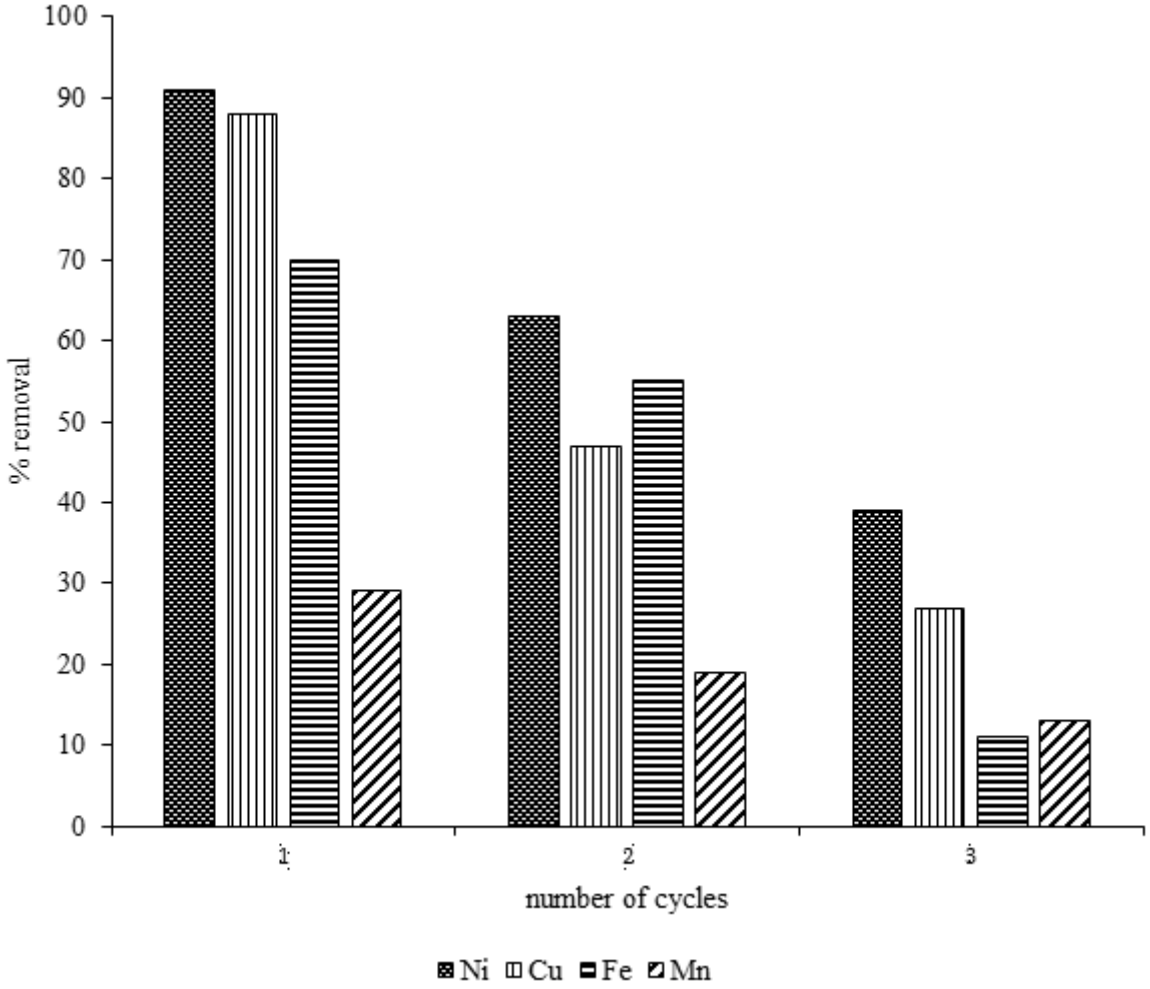

Figure 6

Variation of metal removal with the number of recycles of MO seed extract.

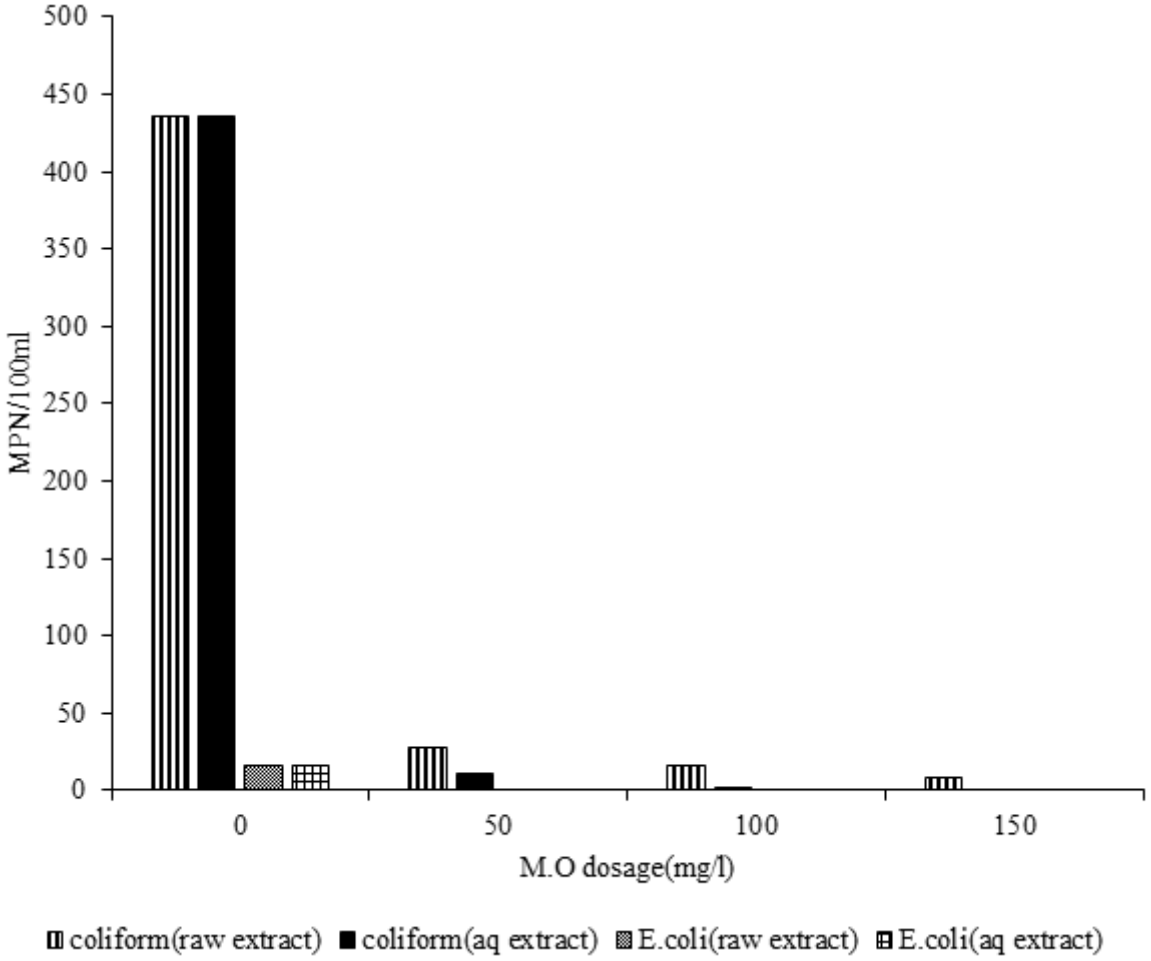

Figure 7

Variation of MPN/100ml of total coliform and E.coli with MO dosage for wastewater treated with raw extract and aqueous extract.

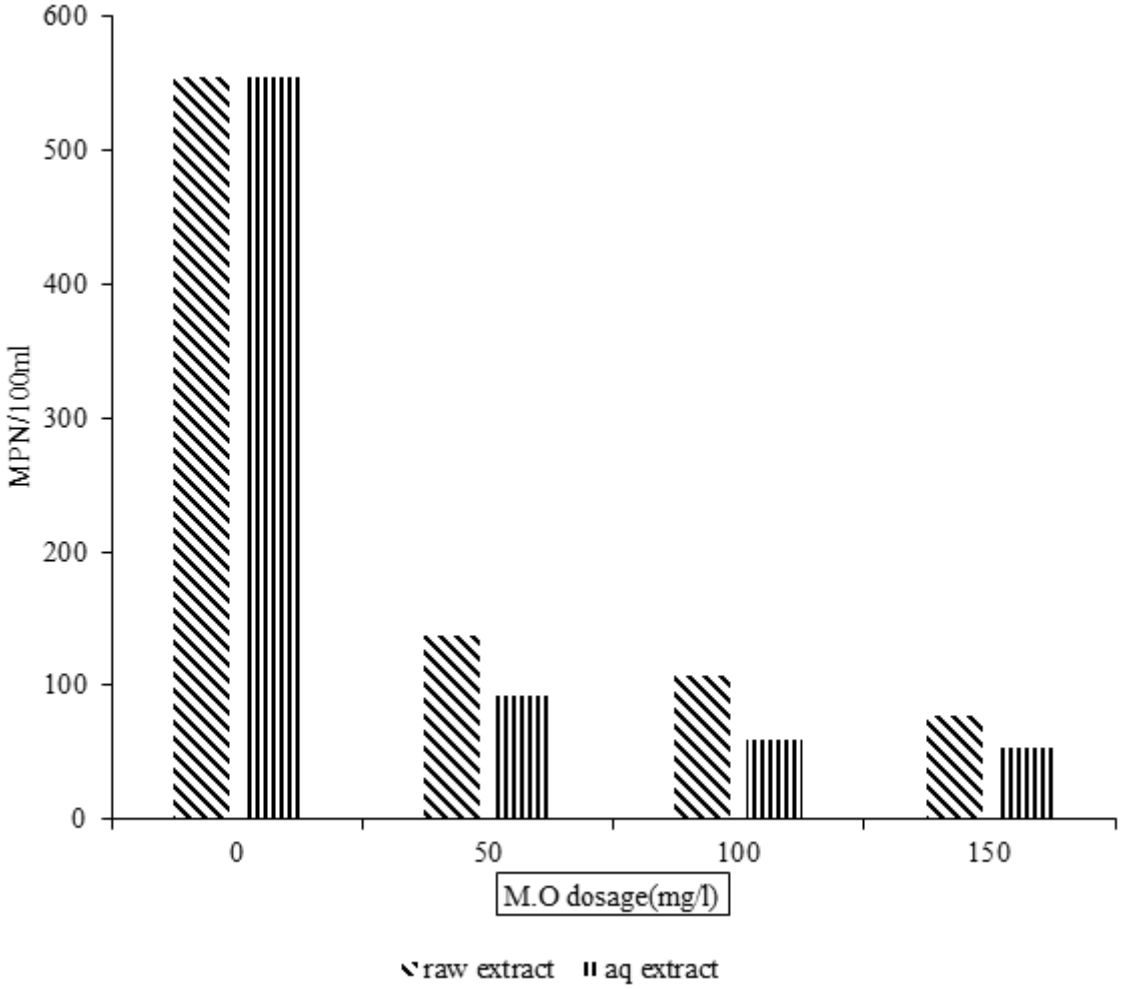

Figure 8

Variation of MPN/100ml with MO dosage for wastewater treated with raw and aqueous extracts.

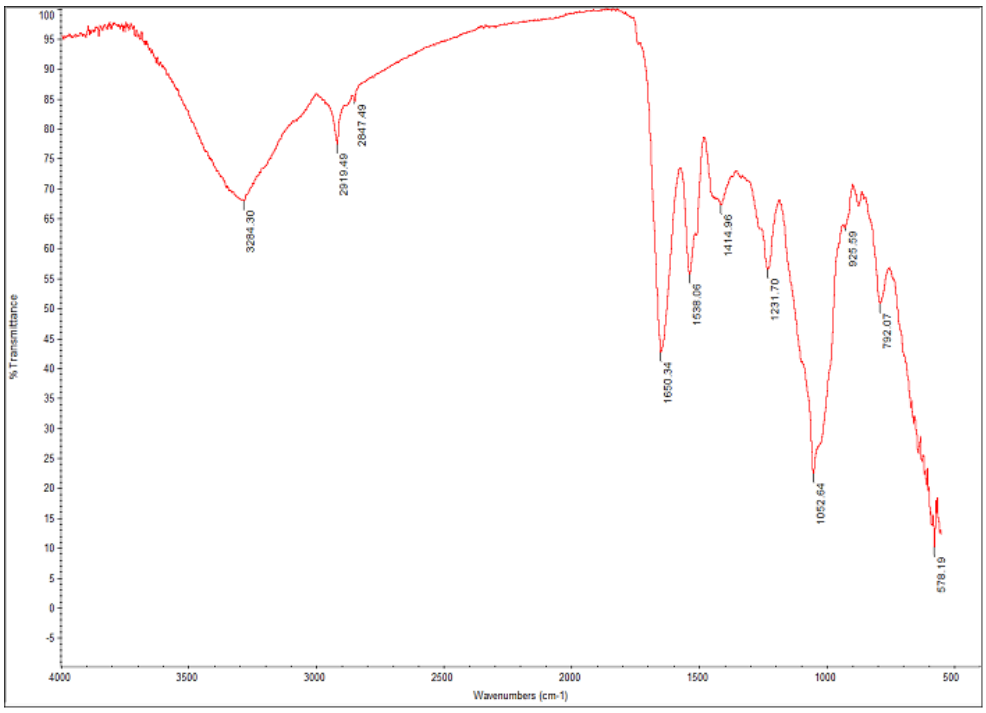

(a)

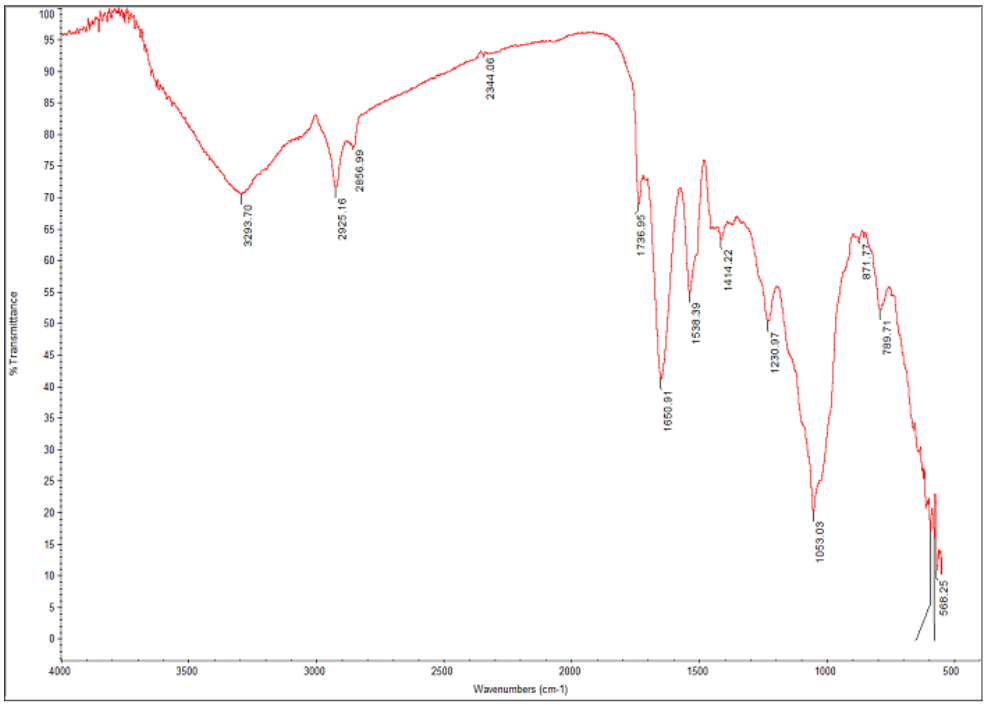

(b)

Figure 9

FTIR spectrum (a) before metal loading (b) after metal loading

Supplementary Files

This is a list of supplementary files associated with this preprint. Click to download.

- supplementarydataanovaanalysis.docx
- supplementarydatalangmuirandFreundlichisotherms.docx